RSC Advances

COMMUNICATION

View Article Online
View Journal | View Issue

Cite this: *RSC Adv.*, 2014, **4**, 31652

Received 13th April 2014
Accepted 11th July 2014

DOI: 10.1039/c4ra03350g

www.rsc.org/advances

Electron beam manipulation of gold nanoparticles external to the beam†

Yu-Ting Chen,[a] Chiu-Yen Wang,[b] Ying-Jhan Hong,[a] Yu-Ting Kang,[a] Shih-En Lai,[a] Pin Chang[c] and Tri-Rung Yew*[a]

The electron beam (e-beam) of transmission electron microscopy (TEM) was utilized for *in situ* synthesizing and manipulating Au nanoparticles with various sizes in $HAuCl_4$ aqueous solution. The driving force for e-beam manipulation was found to be a function of particle-to-beam distance, mostly due to the electric force. From experimental observations, it was concluded that the e-beam can attract the Au nanoparticles in the $HAuCl_4$ solution. This contributes to the dipole induced in the Au nanoparticle, which is attributed to the non-uniform positive potential built inside the observation window. On the other hand, this positive potential would induce a repulsion force with the positively charged Au nanoparticle. Therefore, repulsion behaviour of the Au nanoparticle induced by the e-beam was also observed.

Introduction

Nanoparticles have drawn increasing attention over the years through the use of nanoparticle manipulation in fields such as biology, chemistry, engineering, and physics. As a result, many techniques have been developed, *e.g.*, the scanning probe microscopy manipulation,[1,2] optical tweezers,[3,4] acoustic tweezers[5,6] and magnetic tweezers,[7] all designed for various purposes.

Recently, the technique of nanoparticle manipulation by e-beam was proposed to control nanoparticles with sizes only of several nanometers in diameter.[8–11] The e-beam was also used for the observation of samples during or immediately after the manipulation. Oleshko *et al.* were the first to introduce the e-beam for nanoparticle manipulation.[12] In their research, an e-beam was utilized to trap an Al nanoparticle with a size of 20 to 300 nm in molten Al–Si eutectic alloy. The e-beam was able to move the nanoparticle with a displacement of 40 to 100 nm. They proposed that the trapping of nanoparticles inside the e-beam illumination area might be attributed to the momentum transfer from the electrons. It was later concluded that this force due to momentum transfer between a 200 keV electron beam and a 10 nm nanoparticle was actually too small for manipulation. Around the same time, Batson *et al.* proposed another method to manipulate nanoparticles with e-beam.[8,9] A swift e-beam in scanning transmission electron microscopy (STEM) was applied to control the position of Au nanoparticles on an amorphous carbon film. The interaction between the nanoparticle and e-beam was much complicated in this case, as such interaction was sensitive to the distance between nanoparticles and e-beam scanning direction.

With the development of environmental cells,[13] the observation of liquid materials in TEM, STEM and possibly other analytical tools requiring high vacuum have become possible. Zheng *et al.* reported that citrate coated Au nanoparticles dispersed in solution could be trapped in the illumination area of the e-beam using TEM.[10,11] The trapping force of e-beam was directly measured by the probability distribution of the Au nanoparticles from the beam center and was calculated to be 1 pN. Though approached from many aspects, the mechanism of this trapping force remained unknown.

In this study, we provide a new prospect with the influence of an e-beam on nanoparticles outside the e-beam illumination area. The technique of liquid-phase electron beam induced deposition (LP-EBID)[14,15] from the $HAuCl_4$ aqueous solution was utilized for *in situ* synthesizing Au nanoparticles of various sizes. These Au nanoparticles would be slightly attached to the observation window (Si_3N_4 thin film in this study), while free from Brownian motion. Therefore, the particle locations and displacements could be clearly observed.

Experimental

A liquid cell named K-kit,[16] as shown in Fig. 1A, was employed as a specimen holder and the manipulation platform in TEM. The fabrication process of K-kit has been described in detail

[a]*Department of Materials Science and Engineering, National Tsing Hua University, Hsinchu, Taiwan, 30013, Republic of China. E-mail: tryew@mx.nthu.edu.tw; Fax: +886-3-5722366; Tel: +886-936347230*

[b]*Department of Materials Science and Engineering, National Taiwan University of Science and Technology, Taipei, Taiwan, 10607, Republic of China*

[c]*Bio Materials Analyses Technology, 1F, No. 26-2, Tai-Yuen St., Jubei City, Hsinchu County, 302, Taiwan*

† Electronic supplementary information (ESI) available. See DOI: 10.1039/c4ra03350g

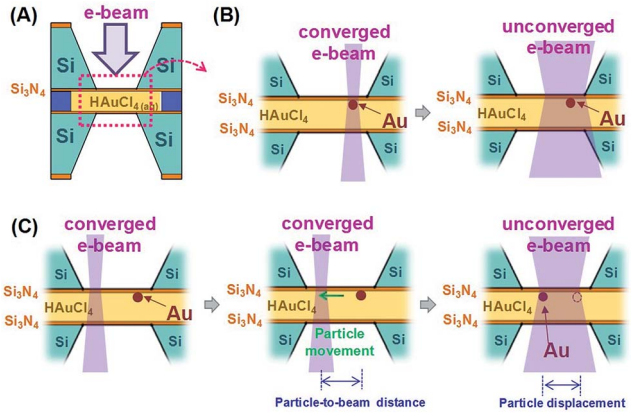

Fig. 1 The schematics of (A) cross-section K-kit, process of (B) *in situ* synthesizing of an Au nanoparticle *via* LP-EBID, and (C) e-beam manipulation of the synthesized Au nanoparticle followed by inspection.

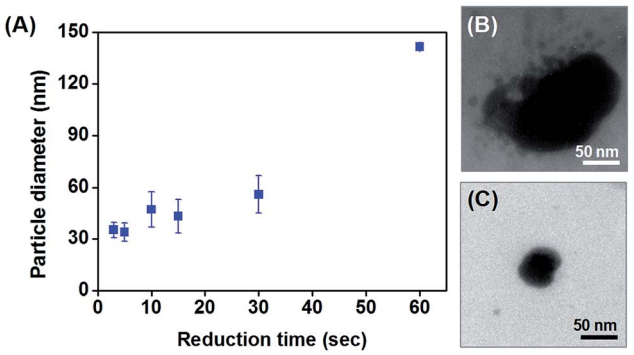

Fig. 2 (A) Plot of Au nanoparticle size *versus* reduction time, and TEM bright field images of Au nanoparticles for reduction time of (B) 60 s and (C) 10 s.

elsewhere.[16,17] The K-kit is basically a liquid sample, a few micrometers thick (5 μm), sandwiched between two pieces of 130 nm Si_3N_4 films which are supported by Si substrates. The 5 mM $HAuCl_4$ aqueous solution (composed of DI water and 99% $HAuCl_4 \cdot 4H_2O$ powder which is purchased from SHOWA) was chosen as a precursor for the LP-EBID of Au nanoparticles. Also, a JEOL 2010 LaB_6 TEM operating at 200 keV was utilized in this study. The e-beam spot size for reduction and manipulation is about 50 nm in diameter under a highly converged e-beam setting.

First, the converged e-beam in TEM for a predetermined time period (reduction time) was used to reduce Au^{3+} in order to form Au nanoparticles. The unconverged e-beam was used to inspect the morphology and size of these nanoparticles as indicated in Fig. 1B. Various particle sizes were obtained by controlling the reduction time of 3, 5, 10, 15, 30 and 60 s. The manipulation sequence is illustrated in Fig. 1C. First, the converged e-beam was located at a chosen distance of 80 nm to 1 μm from the as-reduced Au nanoparticle. Following that, the converged e-beam acted on the nanoparticle for a manipulation time of 10, 20, 30, 45 and 60 s. Unfortunately, the images were not recorded during the manipulation time due to the tightly converged e-beam setting. (The nanoparticles of interest were outside of the e-beam.)

Finally, the position of the Au nanoparticle after the manipulation time would be compared to the position before manipulation, with both recorded under the unconverged e-beam. Consequently, the displacement of the nanoparticle under the influence of the e-beam at various distances from the nanoparticle (defined as "particle-to-beam distances" in the following content) could be determined. The current density of the unconverged e-beam is at least three orders of magnitudes less than that of converged e-beam. Under such current density, the LP-EBID and particle motion caused by e-beam were imperceptible.

Results and discussion

In situ synthesis of gold nanoparticles

As shown in Fig. 2A, the particle size is only weakly related to the reduction time. The x axis represents the reduction time while the y axis the reduced Au nanoparticle diameter which was calculated from the projected area $D = (4A \cdot \pi^{-1})^{1/2}$, where D is particle diameter and A is the particle projected area. With very short reduction time (<5 s), the nanoparticle formed is ~30 nm in diameter, which is of comparable to the e-beam size. Besides, as shown in Fig. 2B and C, the Au nanoparticles reduced are not spherical, suggesting that the particle size and shape are dominated by the e-beam size and the stability of beam location. The small dots (~5 nm) in both figures are believed to be nanoparticles produced by collateral deposition.[14]

E-beam manipulation of *in situ* synthesized gold nanoparticles

Fig. 3 demonstrates the consequence of e-beam manipulation with various particle-to-beam distances. Fig. 3A showed the as-reduced Au nanoparticle with a diameter of 48 nm indicated by the blue arrow. The blue dotted line highlights the original location of this nanoparticle before manipulation. Fig. 3B–F show the results of e-beam manipulation of this Au nanoparticle with an attraction time of 20 s and particle-to-beam distances from 1 μm down to 100 nm. In Fig. 3B–E, the particle-to-beam distances are 790, 600, 470, 420 nm, while the electron beam does not make a detectable movement of the nanoparticle.

However, when the particle-to-beam distance decreased to 360 nm as shown in Fig. 3F, the Au nanoparticle would be attracted to the location of e-beam in 20 s. It should be noted that although the purpose of second converged e-beam illumination was to manipulate the first nanoparticle (blue arrow), a new Au nanoparticle (red arrow) was produced at the beam location through the same LP-EBID process. Since the locations of e-beam in Fig. 3B–F were very close (<200 nm), the new nanoparticle would move with the e-beam. Therefore, this new nanoparticle could be used as a mark of e-beam location. From these results it can be concluded that, for a 48 nm diameter Au nanoparticle, the particle-to-beam distance should be shorter than 360 nm in order to move the nanoparticle.

By the nature of manipulation using a converged e-beam at a distance, the nanoparticle was not illuminated by the manipulating e-beam. Therefore, the nanoparticle could not be imaged

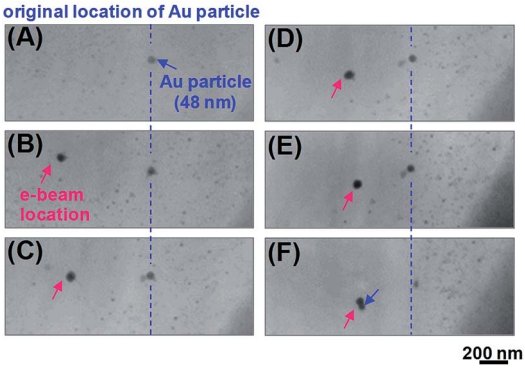

Fig. 3 Sequence TEM bright field images of e-beam manipulation of as-reduced Au nanoparticle: (A) as-reduced Au nanoparticle before manipulation, (B)–(E) Au nanoparticle was not influenced under the particle-to-beam distance of 790, 600, 470, 420 nm and (F) Au nanoparticle was attracted to the e-beam location when the particle-to-beam distance was decreased to 360 nm.

during manipulation time. It needs to rely on the comparison between images before and after manipulation.

A systematic study of the particle displacement in relation to the particle-to-beam distance and to the manipulation time is presented in Fig. 4A. The blue circles, green triangles, and red crosses represent the particle movement of *attracted* to e-beam, *repulsed* from e-beam, and remained *static* under their corresponding particle-to-beam distance, respectively. The attracted and static behavior had been described in the previous paragraph and Fig. 3. When the particle-to-beam distance is further away from attractive force, but not far enough to be stationary, there is a chance for the nanoparticle to be expelled (moved away) from the e-beam. However, the phenomenon of repulsion was not observed in every sample, contrast to that of which attractive and stationary cases are more consistent. From Fig. 4A, it is noted that the distance that e-beam could influence on Au nanoparticle will increase with the increases of attraction time.

Fig. 4B displays the relationship between particle displacement and particle-to-beam distance at different attraction time. For the particle displacement, the positive value was defined as the displacement for attraction, with negative value as repulsion and zero as stationary. Overall, the data points dispersed in the direction of negative slope especially in the range of attraction, suggesting that the driving force for attraction increased as the nanoparticle became closer to the e-beam. This result is consistent with that implied in Fig. 4A. Nonetheless, the dots in Fig. 4B are scattered likely due to uncertainties ($\pm$30 nm) in determining the particle displacements and particle-to-beam distances from the images. In the attraction case, the nanoparticles moved toward the beam and, if given enough time, stopped at the beam location. In other words, the furthest displacement that a nanoparticle can move by e-beam attraction is the particle-to-beam distance. The dashed line in Fig. 4B highlights this limit.

Defined as the particle displacement divided by the corresponding manipulation time, the average velocity in Fig. 4C

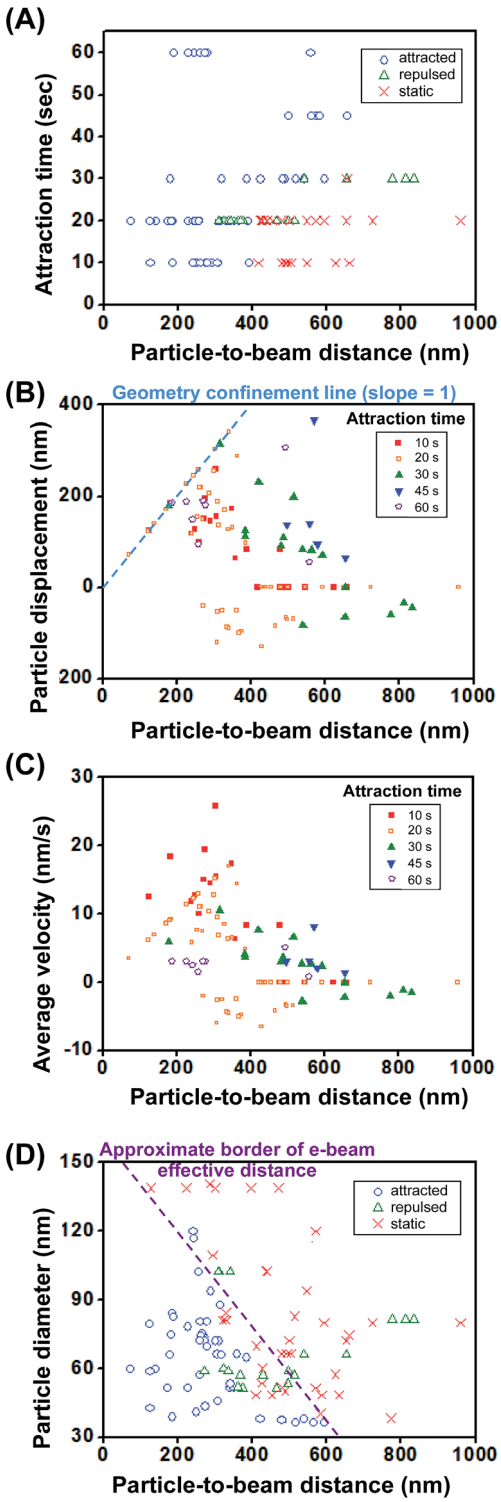

Fig. 4 Plots of (A) e-beam influence, (B) particle displacement, (C) average particle velocity under different attraction time, and (D) e-beam influence under different particle sizes.

tends to be anti-correlated to the particle-to-beam distance. This anti-correlation is not resulted from the particle size variation as shown in ESI 1.† That is to say, the further the nanoparticle was from the e-beam, the slower it moved. However, for

a manipulation time of 60 s, the data points clearly deviated from this trend. As mentioned above, the maximum distance for a nanoparticle to move is particle-to-beam distance. We suspect that 60 s was way too long for the nanoparticles to reach the beam. Therefore, it probably doesn't take all the 60 s for these nanoparticles to be attracted to the beam location. The apparent velocities for these nanoparticles were underestimated.

Meanwhile, it is important to investigate the size of the nanoparticle that the e-beam could move for the practical usage of e-beam manipulation. Fig. 4D illustrates the relationship between particle movement *versus* particle-to-beam distance for various particle sizes. It is easy to observe the farthest distance that e-beam could attract a nanoparticle decreased as the particle size increased. This phenomenon might be explained with Fig. 2B and C. The contact area of Au nanoparticle to the observation window increase with the particle size, which would impede the particle movement.

From these results, it can be concluded that the attractive force declined as the particle-to-beam distance increased. Further away from the beam, under certain circumstance, the repulsive force wins over and the nanoparticle moves away from the beam. When the nanoparticle is far enough, it remain static and not affected by the e-beam. The *in situ* formed Au nanoparticle could be manipulated to any position if the particle size was smaller than 120 nm in diameter and the e-beam moving velocity was slower than 5 nm s^{-1}.

Discussion of e-beam manipulation mechanism

Contrast to Zheng *et al.*'s trapping particles in the e-beam, the nanoparticles we manipulated were some distance outside the e-beam, which makes real time observation impossible. Qualitatively speaking, we speculate that the attraction force is dielectrophoresis (or DEP) and the repulsion force is probably electrostatic force.

It is known that the specimen in TEM will charge up due to loss of electrons through the emission of secondary electrons and auger electrons.[18] Therefore, the silicon nitride window of the K-kit would be positively charged after e-beam illumination. This charge would be shielded by electrolyte in both parallel and perpendicular directions to the window in milliseconds (ESI 2†). However, since the Au nanoparticle would just form underneath the window, it still mainly suffered the built-in electric field in the silicon nitride window. For simplicity, we assume that the window material is uniformly charged in the area under the e-beam illumination (or bombardment). Fig. 5A and B show the sketches of the electric field strength distribution[18] corresponding to the e-beam location with a beam size of 50 nm and 250 nm, respectively. Note that the silicon nitride window thickness is 130 nm and the drawing is not to scale.

We speculate that it is the non-uniform electrical field that attracts Au nanoparticles by di-electrophoretic force, which is proportional to the gradient of the field strength (ESI 3†). Fig. 5C shows two nanoparticles attracted to the (50 nm) e-beam location marked a cross in upper picture before manipulation. The lower picture shows the nanoparticles after manipulation.

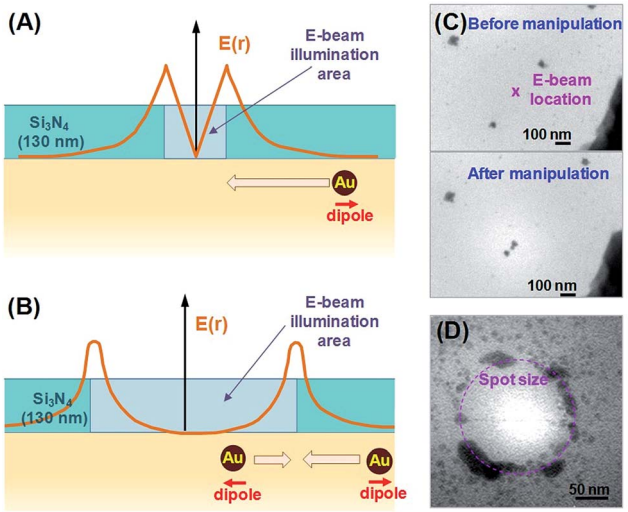

Fig. 5 The schematics of electric field distributed in the observation window and corresponding Au nanoparticle movement because of the dipole generated for (A) spot size smaller than Si_3N_4 thickness and (B) spot size larger than Si_3N_4 thickness, and (C) TEM bright field images of nanoparticles before and after 10 s manipulation with smaller spot size (~50 nm), (D) TEM bright field images of nanoparticles after 10 s manipulation with larger spot size (~250 nm).

Fig. 5D shows the result of large (diameter 250 nm) e-beam for comparison. Clearly, the nanoparticles are attracted to the realm of the e-beam. These results are consistent with the electrical field strength profile in Fig. 5A and B.

As to the repulsion of the nanoparticles, it seems that the only plausible explanation would be related to electrostatic forces. As mentioned before, there is a net charge loss in the liquid when illuminated by the e-beam. In the process for the electrolyte to neutralize local charge imbalance, there is a net flux of positive charges moving away from the e-beam location. It would be possible that the Au nanoparticles are positively charged by chance and the repulsion occurred only for the charged cases. Qualitatively, this picture is consistent with the following observations on the repulsion cases. First, no repulsion observed for 10 s manipulation time, suggesting that is takes some time for this process to take place. Second, it seems to be stochastic, repulsion cases overlap with attraction and stationary cases. However, this picture has difficulty to account for the fact that repulsion takes place at further distances for 30 s manipulation time compared to the 20 s cases. One might be forced to speculate that the repulsion only takes place at the end of e-beam illumination.

Conclusions

In general, the *in situ* formed Au nanoparticle was utilized to study the manipulation ability of e-beam outside the illumination area. The size of this *in situ* synthesized Au nanoparticle could be controlled by the reduction time. And the manipulation capability of e-beam is related to the particle-to-beam distance. With a shorter particle-to-beam distance, the attraction force of e-beam to the nanoparticle was larger.

From experimental results, a mechanism is proposed that the attraction behavior was attributed to the interaction between the built-in electric field in the window and the dipole induced in the Au nanoparticle. The repulsion behavior was speculated to result from the positively charged Au nanoparticles in this electric field. However, this mechanism is still far from complete and more quantitative work should follow. The mechanism of manipulation will be further investigated and the techniques developed in this work can be used for various applications.

References

1 S. Kim, F. Shafiei, D. Ratchford and X. Li, *Nanotechnology*, 2011, **22**, 115301.
2 F. Silly, A. O. Gusev, A. Taleb, M. P. Pileni and F. Charra, *Mater. Sci. Eng., C*, 2002, **19**, 193.
3 D. G. Grier, *Nature*, 2003, **424**, 810.
4 J. R. Moffitt, Y. R. Chemla, S. B. Smith and C. Bustamante, *Annu. Rev. Biochem.*, 2008, **77**, 205.
5 X. Ding, S. C. S. Lin, B. Kiraly, H. Yue, S. Li, I. K. Chiang, J. Shi, S. J. Benkovic and T. J. Huang, *Proc. Natl. Acad. Sci. U. S. A.*, 2012, **109**, 11105.
6 J. Shi, D. Ahmed, X. Mao, S. C. S. Lin, A. Lawit and T. J. Huang, *Lab Chip*, 2009, **9**, 2890.
7 I. De Vlaminck and C. Dekker, *Annu. Rev. Biophys.*, 2012, **41**, 453.
8 P. E. Batson, A. Reyes-Coronado, R. G. Barrera, A. Rivacoba, P. M. Echenique and J. Aizpurua, *Nano Lett.*, 2011, **11**, 3388.
9 P. E. Batson, A. Reyes-Coronado, R. G. Barrera, A. Rivacoba, P. M. Echenique and J. Aizpurua, *Ultramicroscopy*, 2012, **123**, 50.
10 H. Zheng, *Nanoscale*, 2013, **5**, 4070.
11 H. Zheng, U. M. Mirsaidov, L.-W. Wang and P. Matsudaira, *Nano Lett.*, 2012, **12**, 5644.
12 V. P. Oleshko and J. M. Howe, *Ultramicroscopy*, 2011, **111**, 1599.
13 N. de Jonge and F. M. Ross, *Nat. Nanotechnol.*, 2011, **6**, 695.
14 G. Schardein, E. U. Donev and J. T. Hastings, *Nanotechnology*, 2011, **22**, 015301.
15 Y. Liu, X. Chen, K. W. Noh and S. J. Dillon, *Nanotechnology*, 2012, **23**, 385302.
16 K. L. Liu, C. C. Wu, Y. J. Huang, H. L. Peng, H. Y. Chang, P. Chang, L. Hsu and T. R. Yew, *Lab Chip*, 2008, **8**, 1915.
17 L. A. Tai, Y. T. Kang, Y. C. Chen, Y. C. Wang, Y. J. Wang, Y. T. Wu, K. L. Liu, C. Y. Wang, Y. F. Ko, C. Y. Chen, N. C. Huang, J. K. Chen, Y. F. Hsieh, T. R. Yew and C. S. Yang, *Anal. Chem.*, 2012, **84**, 6312.
18 J. Cazaux, *Ultramicroscopy*, 1995, **60**, 411.

